DOI: 10.1002/adsc.200900526

Selective Hydrogenation of 5-Ethoxymethylfurfural over Alumina-Supported Heterogeneous Catalysts

Erik-Jan Ras,[a,b] Sergio Maisuls,[a] Paul Haesakkers,[a] Gert-Jan Gruter,[a,*] and Gadi Rothenberg[b,*]

[a] Avantium Technologies B.V., Zekeringstraat 29, 1014BV Amsterdam, The Netherlands
Fax: (+31)-(0)20-586-8085; phone: (+31)-(0)20-586-8080; e-mail: gert-jan.gruter@avantium.com
[b] Van 't Hoff Institute of Molecular Sciences, University of Amsterdam, Nieuwe Achtergracht 166, 1018 WV Amsterdam, The Netherlands
Fax: (+31)-(0)20-525-5604; phone: (+31)-(0)20-525-6963; e-mail: g.rothenberg@uva.nl

Received: July 29, 2009; Published online: November 24, 2009

Abstract: We report here the synthesis and testing of a set of 48 alumina-supported catalysts for hydrogenation of 5-ethoxymethylfurfural. This catalytic reaction is very important in the context of converting biomass to biofuels. The catalysts are composed of one main metal (gold, copper, iridium, nickel, palladium, platinum, rhodium, ruthenium) and one promoter metal (bismuth, chromium, iron, sodium, tin, tungsten). Using a 16-parallel trickle-flow reactor, we tested all 48 catalyst combinations under a variety of conditions. The results show that both substrate conversion and product selectivity are sensitive towards temperature changes and solvent effects. The best results of >99% yield to the desired product, 5-ethoxymethylfurfuryl alcohol, are obtained using an iridium/chromium (Ir/Cr) catalyst. The mechanistic implications of different possible reaction pathways in this complex hydrogenation system are discussed.

Keywords: bimetallic catalysts; biomass conversion; furfural; iridium; parallel flow reactors

Introduction

In 2008, crude oil prices peaked at over $140 per barrel, promoting a surge of activity towards finding renewable energy solutions. While the price of crude oil has abated somewhat with the financial crisis that followed, long-term availability prognoses remain pessimistic. Indeed, regardless of whether we have already passed the so-called 'peak oil' point or not, the move towards renewable feed stocks will have to be made in our lifetime. Much work is being done in several parallel fields, including harnessing solar,[1] wind,[2]and geothermal power,[3] developing safer nuclear technologies,[4] and refining biomass.[5,6] Of these, biomass refining is the most readily applicable on a large scale worldwide. This is because the current energy market is a conservative one, with companies looking first and foremost for pragmatic solutions. Changing from one energy source to another often requires new and costly infrastructures. In this respect, biomass conversion is less problematic than hydrogen energy, for example, since much of the existing infrastructure can be used. Moreover, there is ample biomass available (we convert today less than 7% of the available biomass to chemicals and energy).

The problem is that biomass is chemically very different from crude oil. Crude oil is composed of hydrocarbons, most of which are unfunctionalized. Biomass, on the other hand, is typically over-functionalized. It is a mixture of alcohols, ethers, esters, and carboxylic acids. Thus, catalytic refining of biomass presents different, and often yet unmet, challenges. Previously, we have studied various catalytic options for valorizing fatty acids,[5] triglycerides,[6] and glycerol derivatives.[7] Here, we focus on furfural derivatives, which can be obtained from cellulose, starch, hemicellulose and sugars.[8] Specifically, we study the catalytic conversion of 5-ethoxymethylfurfural **1** to 5-ethoxymethylfurfuryl alcohol **2** (Scheme 1). This unsaturated alcohol is a potential additive for diesel fuel. Its combustion profile is similar to that of ethanol, yet its miscibility in diesel is much higher. We synthesized and tested a set of 48 bimetallic catalyst combinations supported on γ-alumina, and tested their activity and selectivity in this hydrogenation reaction.

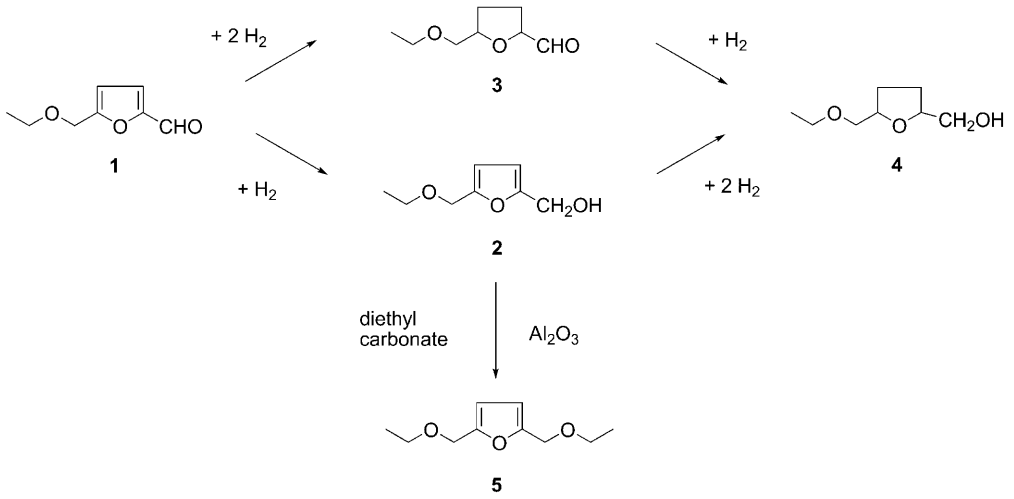

Scheme 1. Catalytic hydrogenation of 5-ethoxymethylfurfural **1**.

Results and Discussion

All hydrogenation reactions were performed in trickle-flow using a 16-parallel flow reactor set-up. In a typical reaction (Scheme 1), a solution of 5-ethoxymethylfurfural **1** was pumped over the catalyst bed together with gaseous H_2. The reactor effluent was depressurized and collected for offline analysis using GC. The main product was 5-ethoxymethylfurfuryl alcohol **2**. By-products included the ring hydrogenated compound **3**, as well as excess hydrogenation compounds such as dimethyltetrahydrofuran, and some oligomers. At higher temperatures, the main product **2** undergoes an etherification with the solvent, diethyl carbonate, giving 2,5-diethoxymethylfuran **5**. This side reaction can be eliminated by using an alternative solvent, 1,4-dioxane (see below).

The starting material is easily obtained *via* a simple acid-catalyzed dehydration of C_6-based sugars, using ethanol as a (co-)solvent. An overview of the acid-catalyzed dehydration of fructose-derived carbohydrates to 5-hydroxymethylfurfural is given elsewhere.[8] However, while the reduction of plain furfural to furfuryl alcohol is easily done in the gas phase,[9–11] 5-hydroxymethylfurfural provides some additional challenges. Its boiling point is much higher compared with furfural (116–118 °C at 11 mmHg and 161.7 °C at 760 mmHg, respectively) (we attempted to measure the boiling point of **2** at atmospheric pressure using DSC and found that decomposition started at 170 °C) yet its thermal stability is lower. This is because the additional electron-withdrawing group facilitates the thermal decarbonylation process

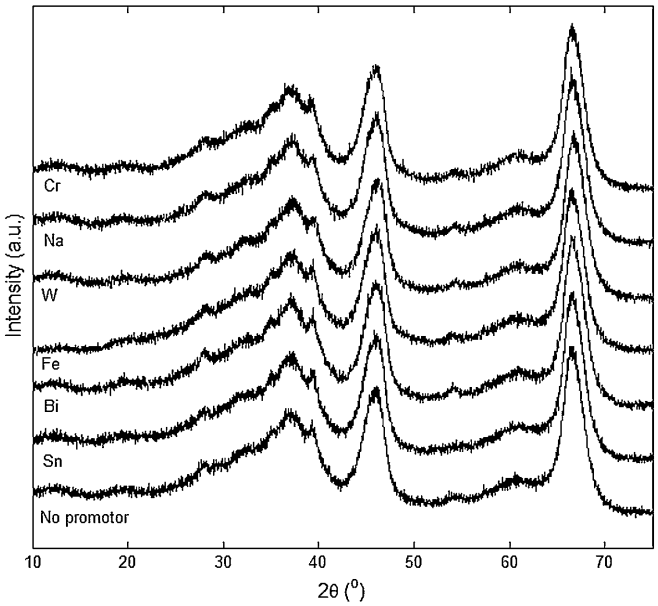

Figure 1. Example XRD patterns obtained for a number of Ir catalyst after calcination. The promoters present have little impact on the properties of the Ir due to their low amounts.

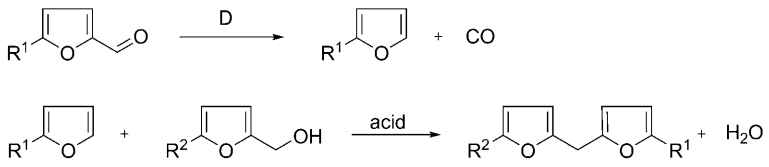

Scheme 2. Thermal decarbonylation of furfural derivatives and dimerisation by electrophilic substitution at the reactive 5-position in the furan ring.

Table 1. Catalyst compositions and key performance data for catalysts B01-B48 tested in diethyl carbonate solvent at 80, 100 and 120 °C.

Entry	Catalyst[a]	80 °C		100 °C		120 °C	
		Conversion [%]	Selectivity[c] [%]	Conversion [%]	Selectivity [%]	Conversion [%]	Selectivity [%]
B01	Au/Bi	33	44	49	20	77	9
B02	Au/Cr	25	33	42	18	73	9
B03	Au/Fe	20	76	53	18	82	8
B04	Au/Na	29	33	43	19	77	8
B05	Au/Sn	37	30	54	16	83	7
B06	Au/W	33	32	50	18	81	8
B07	Cu/Bi	60	17	56	17	53	14
B08	Cu/Cr	67	16	69	13	73	8
B09	Cu/Fe	61	17	59	16	63	10
B10	Cu/Na	61	17	58	18	69	8
B11	Cu/Sn	55	17	53	15	59	9
B12	Cu/W	61	15	53	18	57	12
B13	Ir/Bi	77	73	56	31	68	12
B14	Ir/Cr	95	79	72	31	76	10
B15	Ir/Fe	82	74	57	30	65	13
B16	Ir/Na	91	80	71	25	64	15
B17	Ir/Sn	97	72	66	25	76	7
B18[b]	Ir/W	–	–	–	–	–	–
B19	Ni/Bi	46	21	52	15	45	17
B20	Ni/Cr	37	17	24	29	42	14
B21	Ni/Fe	44	14	26	26	34	16
B22	Ni/Na	47	18	52	12	56	8
B23	Ni/Sn	60	15	64	9	60	9
B24	Ni/W	47	17	54	10	57	8
B25	Pd/Bi	76	18	60	31	94	7
B26	Pd/Cr	100	0	100	16	100	4
B27	Pd/Fe	100	0	100	20	100	6
B28	Pd/Na	100	0	100	0	100	0
B29	Pd/Sn	100	0	100	9	100	1
B30	Pd/W	100	0	100	14	100	5
B31	Pt/Bi	89	71	78	36	98	5
B32	Pt/Cr	91	76	80	30	98	3
B33	Pt/Fe	80	77	70	36	95	6
B34	Pt/Na	86	72	77	25	97	4
B35	Pt/Sn	81	71	73	31	98	3
B36	Pt/W	85	71	75	30	97	4
B37	Rh/Bi	58	60	58	23	89	5
B38	Rh/Cr	76	63	71	22	97	2
B39	Rh/Fe	94	64	89	35	99	3
B40	Rh/Na	78	61	75	20	97	2
B41	Rh/Sn	75	59	65	26	94	4
B42	Rh/W	74	64	72	21	97	3
B43	Ru/Bi	46	30	51	22	69	11
B44	Ru/Cr	46	31	49	21	69	11
B45	Ru/Fe	44	38	50	24	70	12
B46	Ru/Na	43	34	47	23	65	12
B47	Ru/Sn	43	35	45	27	65	14
B48	Ru/W	42	33	42	24	58	14

[a] M1/M2 where M1 = main metal and M2 = promoter. All catalysts Al_2O_3-M1/M2 have a loading of 1 wt% of M1 and 10 mol% of M2 relative to M1.

[b] The experiment with the Al_2O_3-Ir/W catalyst resulted in a blocked reactor, and no performance data could be obtained.

[c] Selectivity denotes the selectivity towards the unsaturated alcohol **2**, calculated as the percentage of the amount of reacted substrate **1**.

(Scheme 2). For this reason, we opted for a liquid phase process, using diethyl carbonate and 1,4-dioxane as solvents. Liquid phase hydrogenation is well established with many examples published.[12,13] We recognize, however, that this choice may facilitate catalyst poisoning by adsorbed CO due to the poor solubility of CO in the liquid phase.

General Trends in Selectivity

A set of 48 bimetallic catalysts (**B1**–**B48**) was prepared *via* excess volume impregnation of porous γ-alumina. Preliminary blank experiments showed that the support itself already exhibited some catalytic activity, thanks to its Lewis acid sites. Aiming to increase activity and optimize selectivity, we synthesized bimetallic catalyst combinations of eight main metals (Au, Cu, Ir, Ni, Pd, Pt, Rh, Ru) at 1 wt% loading, and six promoter metals (Bi, Cr, Fe, Na, Sn, W). In all cases, the promoter loading was 10 mol% relative to the main metal (this enables the study of promoter effects on a molar level). In a typical synthesis, an aliquot of main metal precursor solution and an aliquot of promotor metal precursor solution were added to 1 gram of crushed alumina particles and diluted to a fixed volume of 2 mL. The resulting suspensions were homogenized, dried, calcined and reduced prior to testing their catalytic performance. Whenever possible, we used nitrate precursors (see Experimental Section for details). Table 1 gives the composition and key performance data for all 48 catalysts.

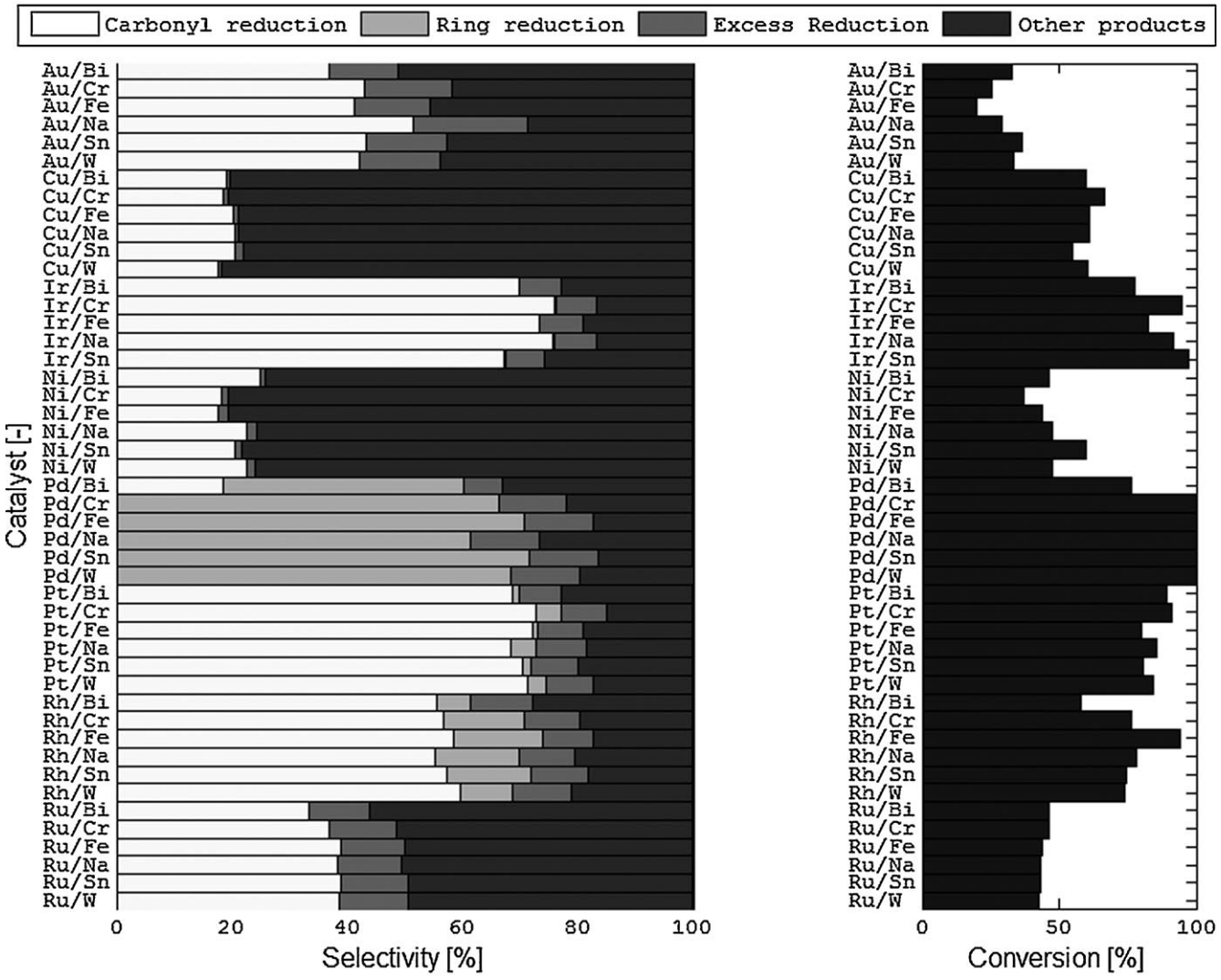

Figure 2. Overview of the selectivity (left) and conversion (right) values obtained at 80 °C in diethyl carbonate. Selectivities shown are grouped as follows: *Carbonyl reduction* (**2**+**5**), *Ring reduction* (**3**), *Excess reduction* (all further hydrogenation products), and *Other products* (i.e., oligomers and unidentified products).

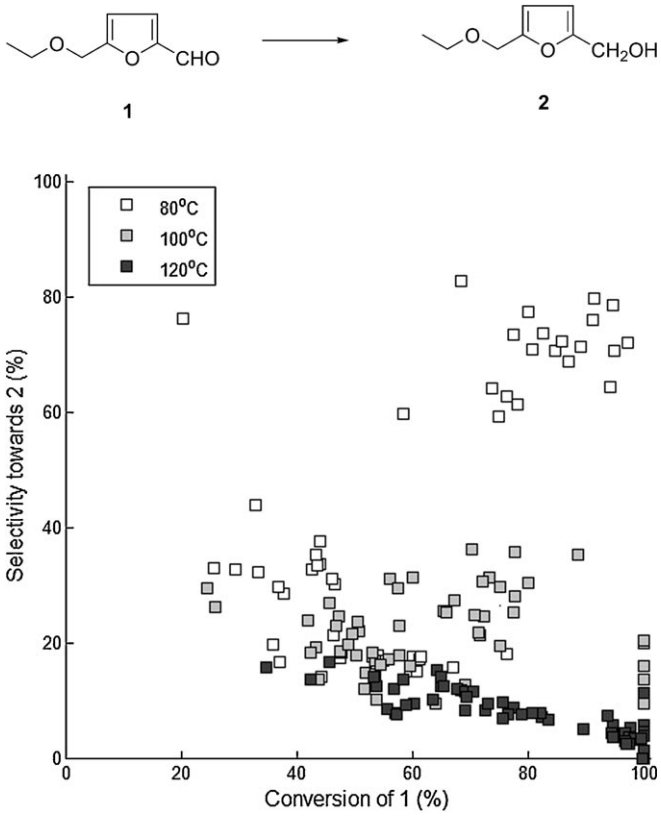

Figure 3. Selectivity towards the unsaturated alcohol **2** *vs.* conversion at three different temperatures, using diethyl carbonate as solvent. Blank experiments using plain alumina tested under the same conditions, conversion levels of 50%-62% and selectivity levels of 6%-15% are obtained.

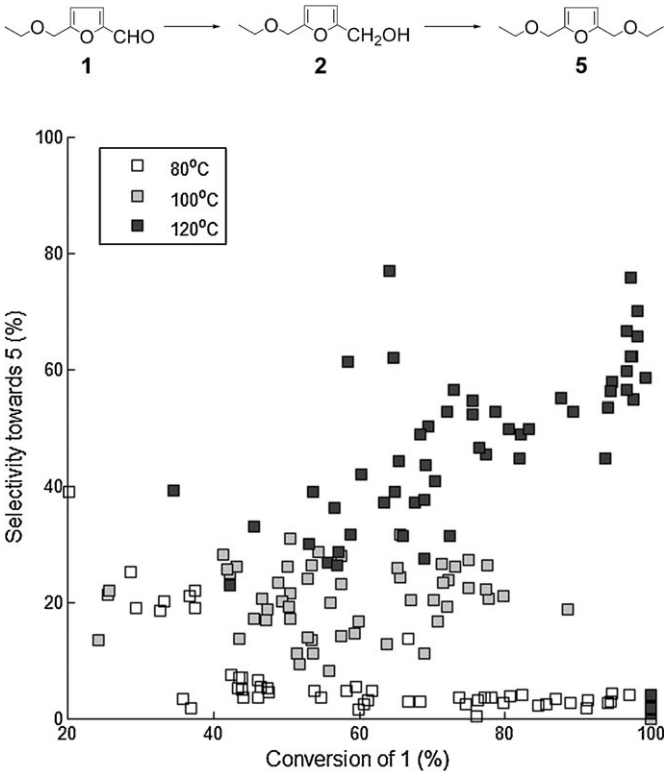

Figure 4. Selectivity towards the etherification product **5** as a function of conversion of **1** at three temperatures. The ethyl group originates from the reaction solvent diethyl carbonate.

To probe the effect of particle size on performance we have analyzed all the catalysts after calcination using X-ray diffraction. The X-ray patterns are nearly identical. We see that there is no impact of the promotors on the particle sizes of the main metal and therefore the X-ray patterns could not provide us with additional insight in the differences or similarities in performance between catalysts. As an example, the patterns obtained for a number of Ir catalysts are given in Figure 1.

Looking at Table 1, we see that the Ir and the Pt catalysts (**B13–B17** and **B31–B37**, respectively) exhibit a much higher selectivity at higher conversion compared to all the other catalysts. For these two main metals, the yield of the Cr-promoted catalysts is somewhat higher than that observerd for other promotors. Interestingly, the Pd-containing catalysts (**B25–B30**) give practically no selectivity to the unsaturated alcohol **2**, but up to 77% selectivity towards the saturated aldehyde **3**. The capability of Pd to reduce C=C double bonds is well known.[14] Figure 2 gives a graphic overview of the product selectivity trends at 80 °C.

Effect of Temperature on Conversion and Selectivity

A well known mechanism for controlling the selectivity in the reduction of carbonyl compounds is changing the reaction temperature.[15] Systems where the selectivity towards alcohol intermediates increases or decreases with temperature are reported. In other cases temperature, has no effect on the selectivity. We observe a decrease in selectivity towards the unsaturated alcohol **2** with temperature. Figure 3 clearly shows this downward trend, where the majority of the points follow an asymptotic selectivity-conversion relationship. The cluster of data with higher selectivities at higher conversions is populated by catalysts containing Ir, Pt and, to a lesser extent, Rh. For these catalysts, a different temperature trend is observed, where not only selectivity but also conversion decrease with temperature. This decreasing conversion with temperature, which seems counter-intuitive at first glance, can be explained by catalyst deactivation at higher temperatures.

A known mechanism for catalyst deactivation in the reduction of aldehydes is the irreversible adsorption of CO on the catalyst surface.[16] The CO in this case originates from decarbonylation of the aldehydes **1** and **3**. Another trend that we see is the increasing

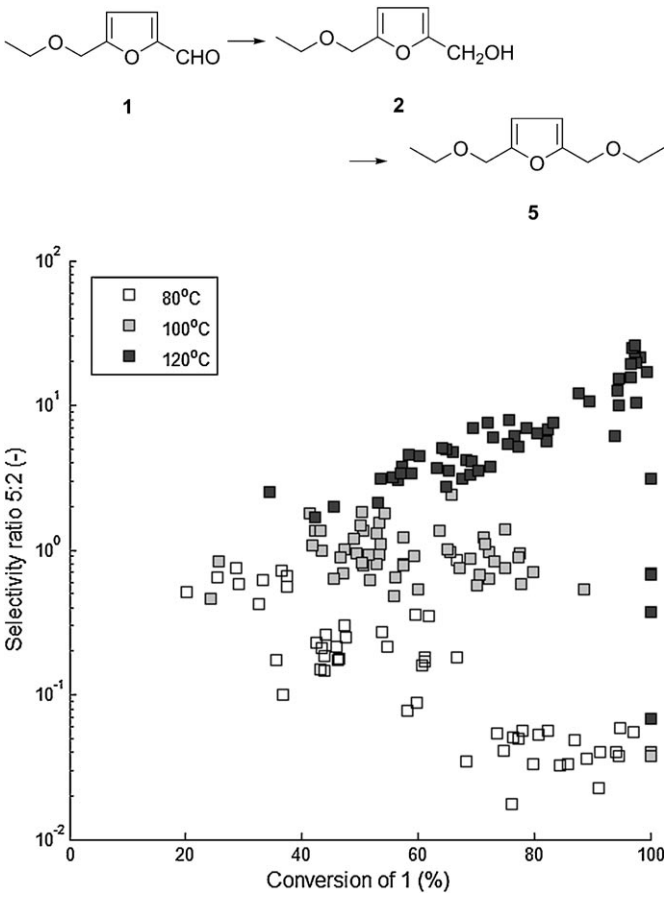

Figure 5. Semilogarithmic plot of the ratio between the selectivities towards the unsaturated alcohol **2** and its ethyl ether **5** as a function of conversion at three temperatures. The apparent outliers at 100 °C and 120 °C are the Pd catalysts which show high selectivity towards the saturated aldehyde **3**.

selectivity towards etherification with increasing temperature. The ethyl ether of the unsaturated alcohol **2**, formed by reaction between **2** and the solvent diethyl carbonate, is formed increasingly at higher temperatures. This reaction is catalyzed by the acidic features of the alumina support. Figure 4 shows the selectivity towards the etherification product **5** as a function of conversion and temperature. Cleary, at 120 °C there is an almost linear relationship between conversion and selectivity towards etherification products. This holds for the majority of the catalysts tested. The role of temperature in the etherification reaction is even more clear when comparing the selectivity ratio between the ether **5** and its precursor **2**. Figure 5 shows this selectivity ratio on a logarithmic scale. Here we see that at 80 °C the etherification product is only formed in substantial amounts at lower conversions and is almost negligible at higher conversions. The effect at 120 °C is opposite, showing a strong increase in the amount of ether **5** being formed at higher conversions. At 100 °C the amounts of unsaturated alcohol **2** and ether **5** are comparable. An alternative route to obtain the diether **5** would be through reduction of diethyl acetal of the aldehyde **1** which is readily formed in ethanol. This option seems a less likely scenario, as fairly large quantities of ethanol are needed in order to yield significant quantities of **5**. Also the conditions required to reduce the acetal, if present, are believed to be more severe than the currently applied conditions. Yet another route to the etherification product was proposed by Milone et al., who explain the formation of cinnamyl ethyl ether in the reduction of cinnamaldehyde by the hydrogenolysis of the hemiacetal.[17] The possible scenarios for our substrate are outlined in Scheme 3.

Excess Hydrogenation

The selective reduction of unsaturated aldhydes is a particularly challenging task, since typically the product of interest is only an intermediate in the overall reaction network. This is true not only in our case, where the goal is selectively hydrogenating the carbonyl bond, but also in cases where selective hydrogenation of the C=C double bond is of interest. The common excess hydrogenation products vary from simple further reduction to fully saturated alcohols. Hydrogenolysis is also observed,[18] where the alcohol formed by carbonyl reduction is cleaved under reductive conditions. In the case of furfural reduction[19] ring opening of the 5-membered ring is observed, mainly after it has been fully reduced.

We observe a variety of excess hydrogenation products, the most prominent are given in Scheme 4. The most abundant product is 2,5-dimethyltetrahydrofuran **9**, which occurs with selectivities up to 40% at 120 °C, mainly with catalysts containing Cu or Ni. The hydrogenolysis products **6** and **8** are observed with selectivities up to 30% at high temperature, most pronounced with Pd catalysts. The fact that larger quantities of **9**, and to a lesser extent 2,5-dimethylfuran **7**, are observed implies that the hydrogenolysis reactions **2**→**6** and **4**→**8** are a lot more common on other metals than one would expect on the basis of the observed selectivities to **6** and **8**. The saturated alcohol **4** is only found in relatively small amounts (up to 5%), when using Pt and Rh as the main metal. This can be explained by the large amount of excess hydrogenation products found.

Effect of Solvent on Catalyst Performance

The major side-product **5** can be attributed to the reactivity of the selected solvent diethyl carbonate. We decided to test 1,4-dioxane as an alternative solvent,

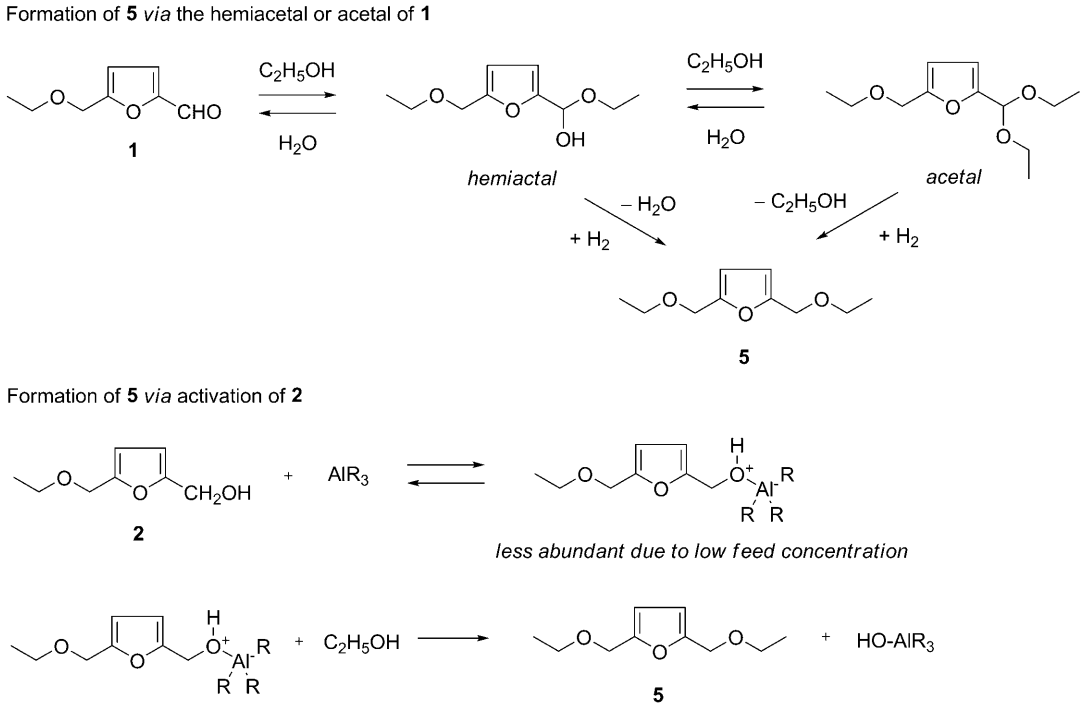

Scheme 3. Possible pathways to the etherification product **5** directly from the substrate **1** and from the unsaturated alcohol **2**. In both cases the source of ethanol is the reaction solvent diethyl carbonate.

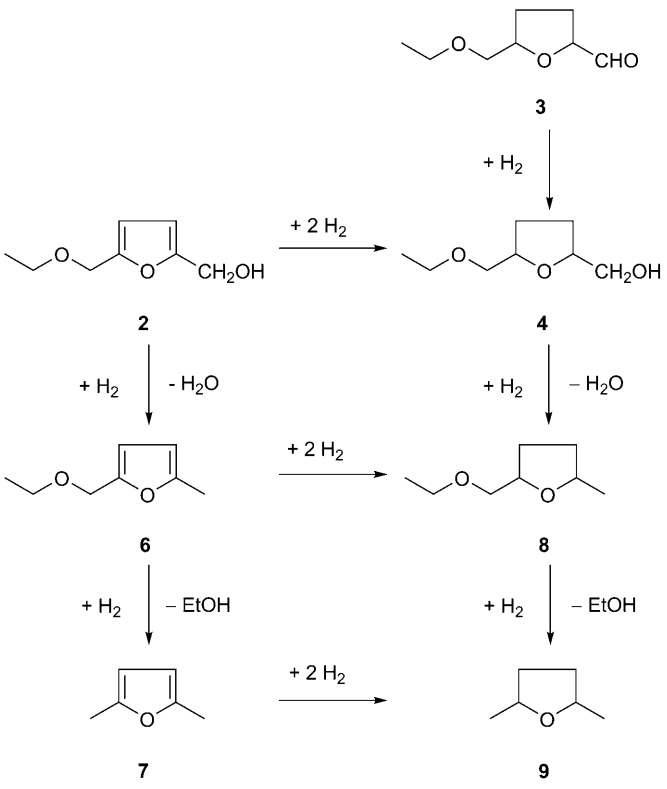

Scheme 4. Excess hydrogenation products originating from selective hydrogenation products **2** and **3**.

to eliminate the reactivity of the solvent. Dioxane was selected due to its similar solvation properties compared to diethyl carbonate for the participants in this reaction. Moreover, 1,4-dioxane is more inert under the applied reaction conditions than diethyl carbonate. Table 2 shows the results of this series of experiments.

The first observation from the results obtained in 1,4-dioxane is the much lower conversion at 80 °C compared with diethyl carbonate. This is explained by the fact that 1,4-dioxane adsorbs more readily to the active sites of the catalysts than diethyl carbonate, due to its electronic structure. Since the substrate is present only in a 1 wt% concentration, this competitive adsorption will favour the solvent over the substrate in most cases. Interestingly, the group of Ir catalysts again shows up as the most successful. This is true both in terms of selectivity towards the desired unsaturated alcohol **2** as well as in terms of the conversion. As expected, the etherification product **5** is not observed in any of the tests, confirming that the ethyl group originates from diethyl carbonate. Whereas the Pd catalysts when tested in diethyl carbonate resulted in almost full selectivity to the saturated aldehyde **3**, experiments in 1,4-dioxane at higher temperatures show that Pd starts to favour the formation of the unsaturated alcohol **2**. This could be explained by a temperature driven change in adsorption mode for the substrate on the catalyst surface. The two

Table 2. Catalyst compositions and key performance data for catalysts B01-B48 tested in 1,4-dioxane solvent at 80, 100 and 120 °C.

Entry	Catalyst	80 °C		100 °C		120 °C	
		Conversion [%]	Selectivity [%]	Conversion [%]	Selectivity [%]	Conversion [%]	Selectivity [%]
B01	Au/Bi	9	42	1	55	0	0
B02	Au/Cr	2	100	9	15	0	0
B03	Au/Fe	9	32	0	0	0	0
B04	Au/Na	6	36	0	0	0	0
B05	Au/Sn	2	100	4	37	0	0
B06	Au/W	7	47	0	0	0	0
B07	Cu/Bi	11	100	5	100	12	100
B08	Cu/Cr	6	100	0	0	0	0
B09	Cu/Fe	6	100	2	67	4	100
B10	Cu/Na	7	100	0	0	5	100
B11	Cu/Sn	5	100	0	0	0	0
B12	Cu/W	7	100	1	100	3	100
B13	Ir/Bi	94	100	44	100	22	100
B14	Ir/Cr	99	100	58	100	25	100
B15	Ir/Fe	92	100	39	100	14	100
B16	Ir/Na	91	100	40	100	12	100
B17	Ir/Sn	95	100	39	100	16	100
B18	Ir/W	98	100	59	100	6	100
B19	Ni/Bi	5	94	0	0	0	0
B20	Ni/Cr	5	96	0	0	0	0
B21	Ni/Fe	0	0	0	0	0	0
B22	Ni/Na	2	100	2	22	0	0
B23	Ni/Sn	2	100	3	22	0	0
B24	Ni/W	0	100	2	27	0	0
B25	Pd/Bi	88	18	26	87	44	81
B26	Pd/Cr	100	0	85	93	94	63
B27	Pd/Fe	100	2	77	70	88	73
B28	Pd/Na	100	1	80	78	93	64
B29	Pd/Sn	99	1	69	94	83	92
B30	Pd/W	100	1	82	87	94	59
B31	Pt/Bi	54	100	18	92	13	100
B32	Pt/Cr	33	97	9	100	26	36
B33	Pt/Fe	35	99	8	100	12	100
B34	Pt/Na	23	99	13	53	21	34
B35	Pt/Sn	18	100	18	46	11	98
B36	Pt/W	38	61	1	100	9	100
B37	Rh/Bi	18	100	0	0	0	0
B38	Rh/Cr	30	100	1	100	0	0
B39	Rh/Fe	48	100	25	100	21	100
B40	Rh/Na	24	100	0	0	0	0
B41	Rh/Sn	28	100	2	100	0	0
B42	Rh/W	25	98	11	85	11	100
B43	Ru/Bi	22	16	5	18	2	38
B44	Ru/Cr	29	13	0	0	0	0
B45	Ru/Fe	22	26	0	0	8	52
B46	Ru/Na	19	40	0	0	0	0
B47	Ru/Sn	20	42	0	0	3	100
B48	Ru/W	20	26	0	0	5	74

likely adsorption modes for the substrate **1** are given in Figure 6.

Another large difference between the data obtained using these two solvents concerns the effect of promotors. Whereas in diethyl carbonate the effect of promotor metals is marginal, in 1,4-dioxane it is substantial. The best example of this is shown by the Pd catalysts tested at 100 °C. In terms of conversion, a low conversion of 26% is obtained with Pd/Bi and a high conversion of 85% is obtained with Pd/Cr. The selectivity, on the other hand, shows a low value of 70% with Pd/Fe and a high value of 94% with Pd/Sn. This

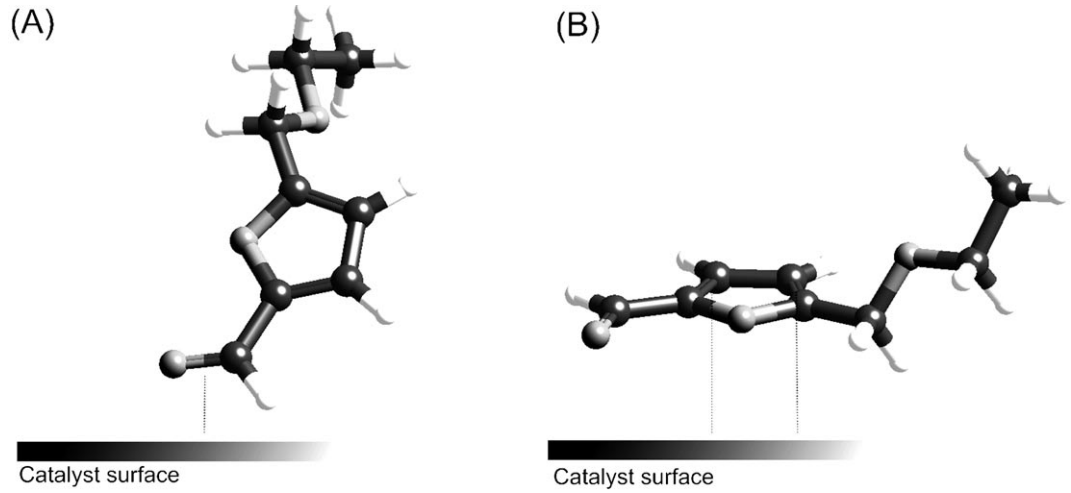

Figure 6. Schematic adsorption modes for the substrate required for (A) carbonyl hydrogenation and (B) ring hydrogenation.

demonstrates that using a more inert solvent like 1,4-dioxane, the effect of promotors is more significant, giving an additional handle for catalyst optimization.

Conclusions

We found that for selectively reducing the carbonyl bond in **1** to yield the unsaturated alcohol **2**, iridium is the most suitable metal supported on γ-alumina. The selectivity and conversion both decrease with temperature, making the choice of experimental conditions the key to success. We also found that Pd supported on γ-alumina is capable of selectively hydrogenating the furan ring in **1**, yielding the saturated aldehyde **3**. This finding is valid only when using diethyl carbonate as solvent. When using 1,4-dioxane as a solvent, also Pd becomes more selective towards **2**. The main side-product observed, when testing the catalysts in diethyl carbonate, is the ethyl ether of the unsaturated alcohol, **5**. The best result in terms of yield of **2** is 99%, using an Ir/Cr catalyst tested in 1,4-dioxane at 80 °C.

Experimental Section

Materials and Instrumentation

X-ray diffraction measurements were performed in the reflection mode using a Bruker machine equiped with a CuK source. Quantitative GC results were obtained using an InterScience TraceGC gas chromatograph equiped with an FID and a VF-WaxMS column (Varian #CP9205; 30 m × 0.25 mm; 0.25 μm stationary phase). The GC program consists of 3 steps: isotherm at 100 °C for 1 min, ramp at 25 °C min^{-1} to 250 °C, isotherm at 250 °C for 3 min. The substrate 5-ethoxymethylfurfural elutes at 3.1 min and the desired product 5-ethoxymethylfurfuryl alcohol elutes at 3.5 min. Identification of unknowns was performed with a Varian GC/MS using the same column and program as above. Spectra were mostly obtained in the EI mode, occas-

Table 3. Precursors used in the synthesis of the catalyst library.

Main metal	Precursor	Promotor metal	Precursor
Au	$HAuCl_4 \cdot 3H_2O$[a]	Bi	$Bi(NO_3)_3 \cdot 5H_2O$[a]
Cu	$Cu(NO_3)_2 \cdot 6H_2O$[a]	Cr	$Cr(NO_3)_3 \cdot 9H_2O$[a]
Ir	$Ir(OAc) \cdot H_2O$[b]	Fe	$Fe(NO_3)_3 \cdot 9H_2O$[a]
Ni	$Ni(NO_3)_2 \cdot 6H_2O$[a]	Na	$NaNO_3$[c]
Pd	$Pd(NO_3)_2$ aqueous solution[c]	Sn	$Sn(OAc)_2$[a]
Pt	$(NH_3)_4Pt(NO_3)_2$[c]	W	$(NH_4)_6W_{12}O_{39} \cdot xH_2O$[a]
Rh	$Rh(NO_3)_3$ aqueous solution[a]		
Ru	$Ru(NO)(NO_3)_3$[c]		

[a] Purchased from Alfa Aesar.
[b] Purchased from Heraeus.
[c] Purchased from Sigma–Aldrich.

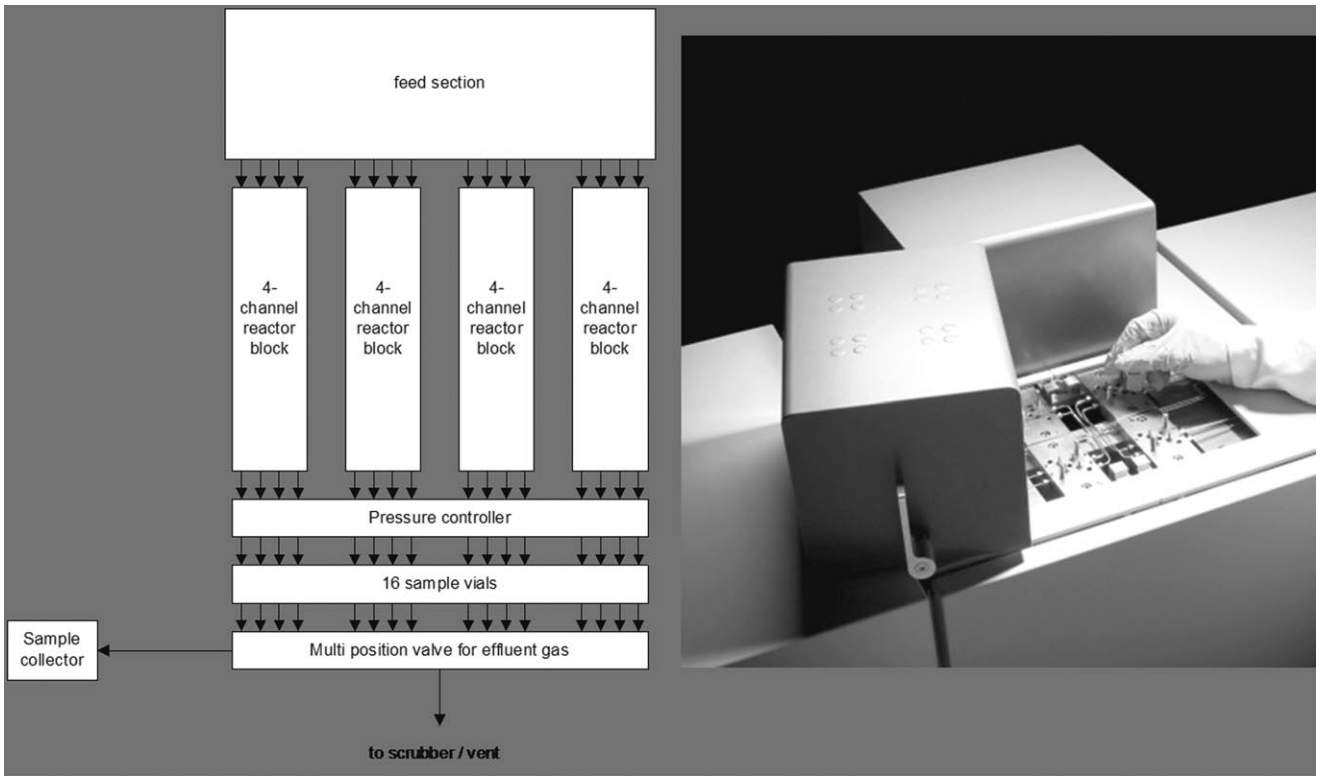

Figure 7. Schematic (*left*) and photograph (*right*) of the 16-channel flow reactor used in this study. This reactor system is supplied commercially by Avantium under the name Flowrence™ (http://www.flowrence.com).

sionally the CI mode was also used. All chemicals were purchased from commercial sources and used as received.

Procedure for Catalyst Synthesis

All catalysts were prepared using wet impregnation. In all cases both metal precursors were impregnated on the catalyst in a single step. Catalyst pretreatment was carried out using the same protocol for all catalysts in the library. The choice for this consistency of preparation recipe is made to eliminate variations in the data due to different recipes being used to generate each catalyst. We acknowledge, however, that some of the catalysts may not have been prepared in the optimal manner. Whenever possible, nitrate precursors were used due to there ease of removal during calcination. An overview of the precursors used and the sources from which they have been obtained is given in Table 3.

Example – Pt/Sn on alumina (B35): A stock solution of tetraamineplatinum(II) nitrate was prepared by dissolving 3.12 g of $(NH_3)_4Pt(NO_3)_2$ in demineralized water in a 25-mL volumetric flask. A second stock solution, of tin(II) acetate, was prepared by dissolving 4.20 g of $Sn(OAc)_2$ in demineralized water using a 10-mL volumetric flask. A few drops of 1 M HCl solution were added to aid dissolution. To 1 g of pre-dried Al_2O_3 (surface area 289 m^2g) support (overnight at 105 °C in air), 160 μL of Pt stock solution and 140 μL of Sn stock solution were added after which the total volume of the system was adjusted to 2 mL. After this the resulting slurry was homogenized for 24 h at ambient conditions. The homogenized sample was dried at 105 °C followed by calcination in air at 320 °C for 16 h. Both temperature increases were achieved using a 5 °C min^{-1} ramp rate. Reduction of the catalyst has been performed in the catalyst test reactor using H_2 (5% H_2 in N_2) at 300 °C and 6 bar for 2 h.

Procedure for Catalyst Testing

All catalysts were tested in a 16-reactor flow setup (Figure 7) using a total liquid feed of 400 μL/min containing 1 wt% substrate and a total gas feed of 25 NmL/min H_2 and 4 NmL/min He (internal standard) at a gas pressure of 6 bar. The combined gas-liquid mixture was distributed over the reactors evenly. In each run an empty reactor was used to evaluate conversion and the remaining 15 reactors contained 50 mg of catalyst, diluted to a bed volume of 100 μL using low surface area zirconia as a diluent. The internal diameter of the reactors is 2 mm. The test protocol consists first of a reduction of the catalysts in the gas phase (5% H_2 in N_2 at 6 bar, 300 °C for 2 h), followed by a three-temperature performance test in trickle phase at 80, 100 and 120 °C. Between the various temperature steps 2 h of equilibration time is allowed before sample collection starts.

Acknowledgements

We thank the Netherlands Organization for Scientific Research (NWO) for funding received under the Casimir programme.

References

[1] B. B. Rath, J. Marder, *Adv. Mater. Processes* **2007**, *165*, 62.
[2] M. Korpas, C. J. Greiner, *Renewable Energy* **2008**, *33*, 1199.
[3] R. Bertani, *Geothermics* **2005**, *34*, 651.
[4] S. David, *Nucl. Phys. A* **2005**, *751*, 429c.
[5] A. A. Kiss, A. C. Dimian, G. Rothenberg, *Adv. Synth. Catal.* **2006**, *348*, 75.
[6] A. A. Kiss, A. C. Dimian, G. Rothenberg, *Energy Fuels* **2008**, *22*, 598.
[7] A. Gordillo, L. Durán Pachón, E. de Jesus, G. Rothenberg, *Adv. Synth. Catal.* **2009**, *351*, 325.
[8] P. Gallezot, *Catal. Today* **2007**, *121*, 76.
[9] B. M. Nagaraja, A. H. Padmasri, B. David Raju, K. S. Rama Rao, *J. Mol. Catal. A: Chemical* **2007**, *265*, 90.
[10] B. M. Reddy, G. K. Reddy, K. N. Rao, A. Khan, I. Ganesh, *J. Mol. Catal. A: Chemical* **2007**, *265*, 276.
[11] J. Wu, Y. Shen, C. Liu, H. Wang, C. Geng, Z. Zhang, *Catal. Commun.* **2005**, 633.
[12] K. T. Hindle, S. D. Jackson, G. Webb, *Curr. Top. Catal.* **2008**, *7*, 115.
[13] E. H. Stitt, R. P. Fishwick, R. Natividad, J. M. Winterbottom, *Catalysis in Application*, in: *Papers presented at the International Symposium on Applied Catalysis*, Glasgow, United Kingdom, July 16–18, **2003**, 153.
[14] S. D. Jackson, A. Monaghan, *Catal. Today* **2007**, *128*, 47.
[15] P. Mäki-Arvela, J. Hájek, T. Salmi, D. Y. Murzin, *Appl. Catal. A: General* **2005**, *292*, 1.
[16] X. Wang, R. Y. Saleh, U. S. Ozkan, *Appl. Catal. A: General* **2005**, *286*, 111.
[17] C. Milone, M. C. Trapani, S. Galvagno, *Appl. Catal. A: General* **2008**, *337*, 163.
[18] X. Wang, R. Y. Saleh, U. S. Ozkan, *J. Catal.* **2005**, *231*, 20.
[19] H.-Y. Zheng, Y.-L. Zhu, B.-T. Teng, Z.-Q. Bai, C.-H. Zhang, H.-W. Xiang, Y.-W. Li, *J. Mol. Catal. A: Chemical* **2006**, *246*, 18.

